Microviscoelastic Moduli of Biomimetic Cell Envelopes

Laurent Limozin,* Alexander Roth, and Erich Sackmann

E22-Biophysik. Physik Department, Technical University of Munich, James Franck Strasse, D-85748 Garching, Germany
(Received 7 February 2005; published 17 October 2005)

Bioanalogue models of composite cell envelopes were designed by electrostatically driven self-assembly of actin shells inside giant vesicles. Viscoelastic relaxation moduli were measured between 0.03 and 20 s as a function of actin density by magnetic bead microrheometry. The shear relaxation spectra exhibited by the composite shells compare well with those of natural cell envelopes and bulk entangled actin networks. Absolute value of the shear modulus was measured for the first time by deformation field mapping. Shear and bending moduli agree well with values obtained by bead fluctuations analysis.

The mechanical behavior of many cells is determined to a large extent by the cell envelope, a composite shell formed by the lipid-protein bilayer (the plasma membrane), and the associated actin-based cytoskeleton, the actin cortex. Judged from micromechanical studies, it behaves as a linear viscoelastic shell [1]. The time dependent cell surface elasticity and viscosity determine the dynamics of cellular processes associated with cellular shape changes, such as cell division [2], adhesion or pseudopod formation [3]. They also determine the time scales over which long range mechanical stresses may be maintained within the cortex before they relax by cytoskeletal reorganizations. Thus, whether the cells behave as tensegrity structures depends on the time scale of the processes considered [4]. A powerful tool to study the viscoelastic behavior of cell envelopes and complex fluids is magnetic bead microrheometry [1,5]. Absolute values of the viscoelastic moduli, surface shear moduli, and viscosities of cell surfaces can be measured, and changes of these parameters by cell stimulating agents can be monitored in real time. Comparison of viscoelastic parameters of cell surfaces and *in vitro* networks of actin [6,7] can yield insight into the structural features of the actin cortex (e.g., mesh size and the degree of cross-linking) [1].

We designed mechanical models of cell surfaces by self-assembly of an actin shell beneath the inner leaflet of giant vesicles of typical diameter of 10 μm [8,9]. Contrary to previous studies where the actin filaments were attached to the outer surface of the vesicles through biotin-streptavidin-biotin linkers [10], the present model was designed by polymerizing actin inside the vesicles and by coupling the filaments to the inner surface of the vesicle through electrostatic forces between actin and lipids exposing positively charged polyethyleneglycol head groups. To measure the viscoelastic impedance of the composite shell, superparamagnetic beads were coupled to the apical cap of the resulting soft shells adhering on glass substrates. Retardation functions $J(t)$ were determined by analyzing the bead deflections evoked by force pulses (acting in the vertical direction) by 3D particle tracking. The in-plane (shearing) and out-of-plane (bending) deformations were evaluated

by assuming spherical symmetry of the top surface of the adhering shells. From the retardation functions, relaxation moduli $G(t)$ were obtained by numerical convolution analysis.

As described in detail previously [9], vesicles with reconstituted actin shells were prepared by electroswelling of a lipid mixture [11] in the presence of low ionic strength G buffer containing 3 μM freshly purified monomeric actin and 3 μM rhodamin-phalloidin (Sigma) for fluorescent studies. Vesicles sedimented and adhered on the bottom of a measuring chamber from which actin in the outer medium was removed by rinsing with pure G buffer. Actin inside the adhering vesicles was polymerized by the addition of 2 mM of Mg^{2+} which diffuse into the vesicles through the ionophore A23187.

The vertical magnetic tweezers setup was mounted on an inverted Zeiss Axiovert 200 microscope equipped with a Plan Neofluar 100x objective and a Hamamatsu ORCA-ER CCD camera working at 30 Hz. The magnetic field gradient was generated with a horseshoe-shaped soft iron core magnetized by two oppositely polarized copper coils, driven by a function generator (Stanford Research) and a homemade power amplifier. The three-dimensional motion of the beads, observed by bright field microscopy, was analyzed with a tracking algorithm as follows. The intensity profile of the bead image was fitted by a two-dimensional Gaussian. The center of the distribution determines the bead position in the image plane (x-y) while its vertical position z is obtained from the Gaussian width $w(z)$. The relationship between the position z of the bead above the focal plane and the width $w(z)$ was determined in a separate experiment [12]. The force was calibrated as a function of the coil current through measurement of the velocity of the beads in water glycerol mixtures of known viscosity. Tosyl activated superparamagnetic beads of 1.4 μm radius (Dynal, Norway) were bound to the vesicle exposing amino functional groups of the polyethylenglycol (PEG) lipid. For each experiment vesicles with only one bead attached to the membrane of the apical hemisphere were chosen. Observation by confocal microscopy showed that the apical hemisphere of the adhering vesicles form to

a good approximation spherical caps. Therefore the position of the magnetic bead can be presented in terms of spherical coordinates (R, θ) with the center of the coordinate system being located in the center of the sphere [Fig. 1(a)]. The horizontal position of the vesicle center and its radius were determined by phase contrast microscopy. The force induced displacement $\vec{x}(t)$ of the beads is, in general, parallel to the plane defined by the meridian and the z axis [plane of drawing in Fig. 1(a)], and deviations from this plane are typically smaller than 0.1 rad. Thus $\vec{x}(t)$ can be decomposed into components $u(t)$ parallel to the meridian (in-plane deformation) and $h(t)$ perpendicular to the membrane surface (out-of-plane deformation).

The creep compliance $J(t) = u(t)/F_{\parallel}$ [or $J(t) = h(t)/F_{\perp}$] was measured by application of sequences of N_p force pulses (typically $N_p \sim 20$) of amplitude F and duration T (typically $T = 32$ s). Each component of the induced displacement (parallel or normal to the vesicle surface) was averaged over the N_p pulses. The creep compliances $J(t)$ were transformed into the relaxation moduli $G(t)$ using the convolution relation [13]

$$\int_0^t J(t - t')G(t')dt' - t = 0 \qquad (1)$$

and the numerical method of Liu [14].

Figure 1(c) provides strong evidence that the polymerized actin forms a thin shell beneath the inner leaflet of the membrane. Figure 1(b) shows that the actin filaments form parallel bands that rarely cross, strongly suggesting that the actin shell is approximately a monolayer. Further evidence for this comes from separate neutron reflectivity measurements of the average thickness and actin density of an actin layer adhering to a lipid monolayer (at the air-water interface) containing 5 mol % DPPE-PEG$_{2000}$-amine [15]. Neglecting residual G actin in the vesicle, the average surface density of actin ρ can be determined according to

$\rho = cR/3$ where R is the radius of the vesicle and c is the initial actin concentration. The linear increase of ρ with the vesicle radius was confirmed by separate measurements of the relative lateral actin density based on the analysis of fluorescence micrographs (unpublished data). The linear relationship allowed us to measure viscoelastic parameters as a function of the actin surface concentration by keeping the initial actin concentration constant and choosing vesicles of different radii. One estimates the average distance ξ between filaments (corresponding to the mesh size of bulk networks) according to $\xi = 1/\rho N_A l$, where $l \simeq 2.8$ nm is the monomer-monomer distance, N_A is Avogadro's number, and the actin density ρ is measured in mol/m^2. For the vesicle of Fig. 1(b) with $\rho = 20$ nmol/m^2 one finds $\xi \simeq 30$ nm, a value much smaller than the lateral resolution of the microscope. Since in Fig. 1(b) filamentous structures are clearly visible, it is likely that actin filaments are locally coupled and assembled into bundles.

Creep response curves $J(t)$ were measured for forces ranging from 0.6 to 3.4 pN. As shown in the example of Fig. 2, all curves slow down and tend to saturate at $t > 10$ s. Careful observations of the vesicle shape by phase contrast microscopy showed that no appreciable global deformation is induced by the applied forces, showing that the induced bead deflection is due to local deformation of the shell. The local deformations of the vesicle shell were fully reversible.

For further evaluation we consider the relaxation modulus $G(t)$ obtained from $J(t)$ by convolution (Fig. 2). The relaxation moduli exhibit a characteristic shape consisting of four distinct regimes. At short times $G(t)$ relaxes rapidly with time. At $t > \tau_1$ a crossover into a plateau regime is
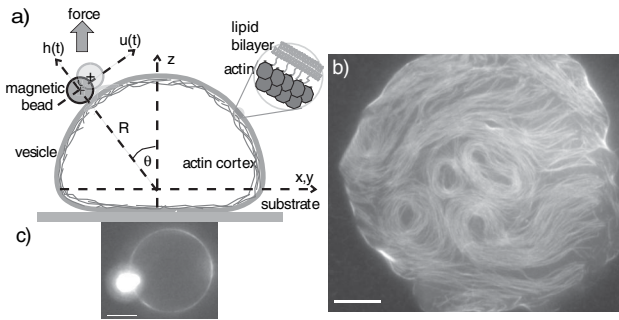

FIG. 1. (a) Schematic side view of a composite actin-membrane shell adhering on a substrate. Force induced deflections of the magnetic bead are decomposed into components parallel (u) and perpendicular (h) to the vesicle surface. (b),(c) Fluorescence micrograph of actin cortex taken by focusing onto an adhering area of the vesicle shell (b) or at the equator of a vesicle (c). The bright object in (c) is the magnetic bead adhered to the vesicle surface. Scale bar: 5 μm.
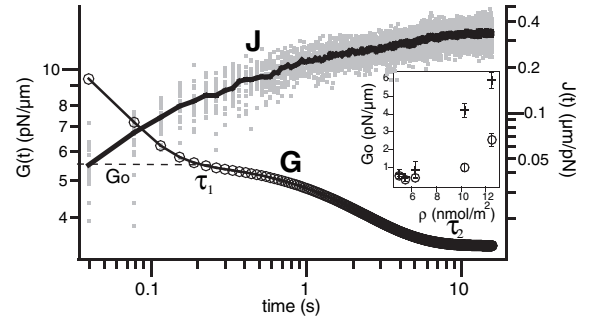

FIG. 2. Averaged in-plane creep compliance $J(t)$ (raw data points shown in gray) and corresponding calculated relaxation modulus $G(t)$ of vesicle with actin surface concentration of 12 nmol/m^2 for an applied force $F = 1.8$ pN. Note four regimes of $G(t)$ (see text for details). Inset: Variation of in-plane plateau modulus G_0 (crosses) and elastic constant k (circles) obtained from the analysis of the thermal fluctuations of the beads as a function of actin cortex density ρ (corresponding to vesicles of various diameter). Error bars represent the standard deviation of G_0 and k determined for different forces and methodological uncertainties.

observed, which goes over into a flowlike behavior at $t \gg \tau_1$ and finally ends in a second plateau at $t > 10$ s. Apart from the second plateau regime, the relaxation modulus of the composite actin-membrane shell closely resembles that of entangled or weakly cross-linked actin solutions [7]. The transition time $\tau_1 \sim 0.15$ s is of the order of the entanglement time of the entangled actin networks solution, which is typically $\tau_e \sim 0.3$ s. We thus identify the short time regime with the relaxation of the filament tension and the plateau at $t > \tau_1$ with the affine deformation of the actin cortex. The plateau modulus G_0 is thus a measure for the shear elastic modulus of the actin cortex. The terminal regime at $t > \tau_2$ does not correspond to the normal flow by reptation diffusion as indicated by the appearance of a second plateau. Figure 2 (inset) shows that the in-plane plateau modulus G_0 increases monotonically with surface actin density ρ. Because of the small variation of density, the present data are compatible either with a quadratic dependence, as suggested for bulk networks [7], or with a linear dependence starting at $\rho > 6$ nmol/m^2. This points again to substantial coupling of the actin filaments, which determines also the shear elasticity.

In the absence of external forces the beads exhibited remarkable in-plane and out-of-plane thermal fluctuations. We measured the mean square displacement $\langle x^2 \rangle$ in each direction by fitting the distribution of the fluctuation amplitudes with a Gaussian function. In the inset of Fig. 2, we plot the effective elastic constants $k = k_B T / \langle x^2 \rangle$ obtained from the mean square amplitudes of the in-plane thermal fluctuations of the bead. Similar to the plateau modulus G_0 the k values increase with the actin density but with a smaller slope. Very similar to the behavior found for the tangential deformations, the out-of-plane relaxation moduli exhibit a plateaulike regime (data not shown) and the plateau value is taken as the measure for the bending modulus of the composite actin-membrane shell.

In order to compare elastic parameters obtained for different model systems such as vesicles with an outer actin coat [10], bulk entangled and cross-linked actin solutions [7], or cell envelopes [1], we determine in the following the bending modulus κ and the surface shear modulus $\mu*$ of the composite shell. Consider first the bending deformation. The pronounced random motion in the normal direction suggests that the tension of the composite shell is small and the out-of-plane deformation is dominated by bending elasticity. The deflection h by a pointlike normal force F is approximately given by [16] $F/h \simeq 8\pi\kappa/R^2 \simeq G_0^h$ where κ is the bending modulus, R the vesicle radius, and G_0^h the out-of-plane plateau modulus. For a vesicle of $R = 6$ μm a value of $G_0^h \simeq 3 \times 10^{-6}$ N/m was found, yielding $\kappa \simeq 4 \times 10^{-18} J \simeq 1000 k_B T$. This value of κ is comparable to the bending modulus found for vesicles coated with an outer layer of actin by analyzing the power spectrum of thermal fluctuations [10]. It is 2 times larger than the bending modulus

measured for the cell envelope of *D. Discoideum* amoeba cells by microinterferometry [17].

A completely different approach to determine bending moduli is by measuring the mean square displacements $\langle h^2 \rangle$ of the out-of-plane thermal fluctuations of the bead. The out-of-plane fluctuations are determined by the overdamped bending undulations of the composite shell. If we neglect the unknown tension of the shell, the mean square amplitude can be related to the bending stiffness κ according to [18] $\langle h^2 \rangle \simeq k_B T R^2 / (2\pi\kappa)$. The measurement of the out-of-plane mean square fluctuations for a vesicle with $R = 6$ μm yielded $\langle h^2 \rangle \sim 8100$ nm^2, which corresponds to a bending modulus $\kappa \sim 700 k_B T$. This value agrees well with that obtained from the plateau modulus of the out-of-plane relaxation modulus.

Consider now the shear deformation. To determine the absolute values of the shear modulus of the composite shell, the deformation field induced by a local (pointlike) force must be known [1]. For this purpose, nonmagnetic polystyrene beads of 0.5 μm radius were coupled to the vesicle surface in addition to the magnetic bead (Fig. 3). The displacements u of the force probes induced by the deflection of the magnetic bead were analyzed as a function of the distance r from the point force. As shown in the inset of Fig. 3, three beads (indicated by a star) exhibit very similar displacements at different distances and are probably connected to a single actin bundle. The displacements of all other beads decrease roughly logarithmically with distance r, with a slope of about 4×10^{-7} m. Considering the shell as a homogeneous elastic sheet of thickness d, the deformation field $u(r)$ induced by a tangential pointlike force F [19], is expected to decay with the distance r from the point of application of the force as $u(r) \simeq F(\ln r_0/r)/(4\pi\mu d)$. F/d is the force per unit length, r is the radial distance from the origin and r_0 is the radius of the
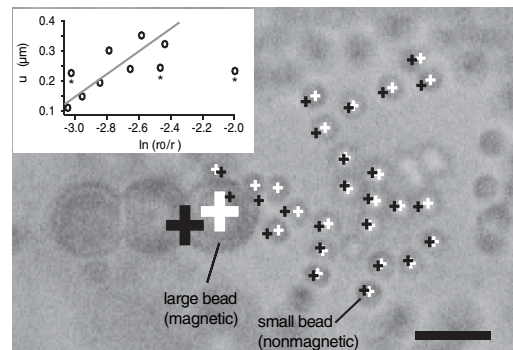
FIG. 3.   Deformation field mapping experiment: Phase contrast micrograph of position of magnetic (large) and nonmagnetic (small) beads on the top hemisphere of a vesicle of radius 16 μm. Black (or white) crosses indicate positions in a force free state (or when a force of 1.8 pN is applied to the magnetic bead). Inset: Plot of the displacement u of force probes as a function of the logarithm of r, the radial distance from the point force. Scale bar: 2 μm.

contact between bead and membrane. μ is the bulk shear modulus (in Pa). According to Fig. 3 (inset), this relation is reasonably well verified. The deformation field decays to about $1/3$ of its maximum value $u(r_0)$ at a distance $\zeta \sim 6~\mu$m, defined as the decay length. The homogeneous shell model should be considered as a zero order approximation since the filaments are locally aligned over distances of several μm. Its application is justified by the finding that the filaments are locally connected. Considering the case of $F = 1.8$ pN, one obtains for the surface shear modulus $\mu^* = \mu d \simeq 4 \times 10^{-7}$ Pa m and for the Young modulus $E = \mu^*/d \sim 50$ Pa by assuming that the shell thickness corresponds to one actin monolayer of thickness $d = 8$ nm [15].

The shear modulus μ can also be estimated from the in-plane thermal fluctuations. Since the membrane is essentially incompressible, the tangential mean square fluctuations associated with shearing are related to μ according to [18] $\langle u^2 \rangle \simeq k_B T (\ln R/a)/(4\pi\mu d)$ where π/a is the largest and π/R the smallest wave vector excited. For a $R = 6~\mu$m vesicle, we measured mean square fluctuations of $\langle u^2 \rangle \simeq 1.2 \times 10^4$ nm^2. By assuming that a is of the order of the interfilament distance $\xi \sim 100$ nm, it yields a surface shear modulus of $\mu^* \simeq 1.1 \times 10^{-7}$ Pa m. This compares well with the value ($\mu^* \simeq 4 \times 10^{-7}$ Pa m) found for a vesicle of $R = 16~\mu$m radius (Fig. 3), which is larger by a factor of 3 if we take into account the dependence on actin density suggested by Fig. 2 (inset).

The observed variation of the shear modulus with the surface actin density (Fig. 2) is qualitatively consistent with laws for entangled or slightly cross-linked tridimensional actin networks [7]. It is thus interesting to compare the elastic moduli of various actin networks. The Young modulus of a vesicle shell exhibiting an interfilament distance of $\xi = 40$ nm (cf. Fig. 3) is $E = 50$ Pa. It is astonishingly similar to the shear modulus of a bulk entangled network of mesh size $\xi = 40$ nm which would be about 60 Pa. The above value for the composite actin-membrane shell is only a factor of 10 smaller than the Young modulus of the envelope of quiescent endothelial cells ($E \sim 400$ Pa [1]) which exhibit a mesh size of the order of $\xi \simeq 100$ nm and a thickness of $\sim 1~\mu$m. This suggests that actin cortices of quiescent cells are only slightly cross-linked as conjectured in a recent study of the viscoelastic impedance of endothelial cells [1]. A next step would be to extend the present study to reconstituted actin cortices cross-linked by proteins [20]. We propose comparative rheological studies of cell models and cell surfaces as a valuable tool to gain insight into structural features of the actin cortex. Giant vesicles with reconstituted actin cortex are examples of soft polymerized membranes exhibiting both bending and shear rigidity. They constitute experimental verifications of statistical surfaces with shear rigidity, which have been extensively studied theoretically [18,21], while quantitative experimental studies of their viscoelastic properties are still scarce.

*Electronic address: limozin@marseille.inserm.fr
†Present address: Cellular Adhesion Group, CNRS FRE2059 Inserm U600, Hospital Sainte-Marguerite, BP 29, 13274 Marseille Cedex 09, France.

[1] W. Feneberg et al., Biophys. J. **87**, 1338 (2004).
[2] K. D. Girard et al., EMBO J. **23**, 1536 (2004).
[3] T. Bretschneider et al., Curr. Biol. **14**, 1 (2004).
[4] D. E. Ingber, J. Appl. Physiol. **89**, 1663 (2000).
[5] A. R. Bausch et al., Biophys. J. **75**, 2038 (1998); B. Fabry et al., Phys. Rev. Lett. **87**, 148102 (2001).
[6] D. C. Morse, Macromolecules **31**, 7044 (1998).
[7] F. C. Mackintosh et al., Phys. Rev. Lett. **75**, 4425 (1995); B. Hinner et al., Phys. Rev. Lett. **81**, 2614 (1998); J. Y. Xu et al., J. Biol. Chem. **273**, 9570 (1998); M. L. Gardel et al., Phys. Rev. Lett. **91**, 158302 (2003).
[8] W. Haeckl et al., Phys. Rev. Lett. **80**, 1786 (1998).
[9] L. Limozin et al., Eur. Phys. J. E **10**, 319 (2003).
[10] E. Helfer et al., Phys. Rev. Lett. **85**, 457 (2000).
[11] Membrane composition: 77.5 mol % DMPC (dimyristoyl-phosphatidylcholine), 17 mol % cholesterol, 3 mol % DPPE-PEG$_{2000}$-amine (dipalmitoylphosphatidylethanolamine-polyethyleneoxide 2000-amine) (all products from Avanti, Al.) and 2.5 mol % ionophore A23187 (Sigma).
[12] A. Roth, Ph.D. thesis, Technical University of Munich, 2004.
[13] N. W. Tschoegl, *The Phenomenological Theory of Linear Viscoelastic Behavior* (Springer, Heidelberg, 1989).
[14] Y. K. Liu, Rheol. Acta **40**, 256 (2001); J. Uhde, Ph.D. thesis, Technical University of Munich, 2004; $G(t)$ is expressed as a sum of exponentials $G(t) = \sum_i g_i \exp(-t/\tau_i)$. The relaxation times τ_i are chosen arbitrarily while the amplitudes g_i are considered as variables. The g_i are determined numerically by minimizing the left-hand side of [Eq. (1)] with the condition $g_i \gtrsim 0$. A typical relaxation time series is defined by $\tau_i = \tau_0 \kappa^i$, with $\tau_0 = 0.00017$ s, $\kappa = 1.2$, and $\tau_{max} = 10000$ s.
[15] K. Sengupta and L. Limozin (unpublished).
[16] L. D. Landau and E. M. Lifschitz, *Theory of Elasticity* (Pergamon Press, Oxford, 1986), 3rd ed.
[17] R. Merkel et al., Biophys. J. **79**, 707 (2000).
[18] P. M. Chaikin and T. C. Lubensky, *Principles of Condensed Matter Physics* (Cambridge University Press, Cambridge, U.K., 1998).
[19] A. E. H. Love, *A Treatise on the Mathematical Theory of Elasticity* (Dover Publications, New York, 1944).
[20] L. Limozin and E. Sackmann, Phys. Rev. Lett. **89**, 168103 (2002).
[21] E. Frey and D. R. Nelson, J. Phys. I (France) **1**, 1715 (1991); R. Goetz et al., Phys. Rev. Lett. **82**, 221 (1999); N. Gov et al., Phys. Rev. Lett. **90**, 228101 (2003).